Mode conversion and the electron-phonon distribution in nonequilibrium metal films

N. Perrin
Groupe de Physique des Solides de l'Ecole Normale Supérieure, 24 rue Lhomond, 75231 Paris CEDEX 05, France

M. N. Wybourne
Department of Physics, University of Oregon, Eugene, Oregon 97403-1274

J. K. Wigmore
Department of Physics, University of Lancaster, Bailrigg, Lancaster LA1 4YB, United Kingdom

(Received 25 April 1989)

We present a model to describe the phonon distribution injected into a solid from a heated metal film in which spontaneous phonon decay is present. The phonon-decay processes are shown to have three main effects: First, after excitation of the metal film the characteristic temperature of the electron distribution is lower than predicted by other models; secondly, the high-frequency component of the longitudinal-phonon spectrum is attenuated; and thirdly, a nonequilibrium transverse-phonon spectrum is generated. We discuss the dependence of these effects on the electric field applied to the film and show that the results are consistent with the available experimental data.

INTRODUCTION

Since the early work of von Gutfeld,[1] heat-pulse measurements have been used by many to study the properties of phonon propagation in solids.[2,3] In these experiments a metal film of thickness d is deposited onto a substrate and is heated either electrically or optically. In both cases, the energy delivered to the electrons is dissipated to the phonons producing a heat pulse. The acoustic-mismatch model[4] was the first attempt to describe the injection of phonons into a solid from a heated metal film. In this model it was assumed that the phonons leaving the film followed a Bose-Einstein distribution with an associated temperature determined by a balance between the electrical power into the film and the loss of phonons from the film. Later, Maris[5] and Perrin and Budd[6,7] introduced a more realistic model describing the distribution of phonons escaping from the film by taking into account the frequency dependence of the electron-phonon interaction in the metal. This model predicted a phonon distribution that differed significantly from a Bose-Einstein distribution.

Summarizing the arguments of the Perrin-Budd model, an electric field applied to a metal film heats the electrons above the lattice temperature and, assuming the electron-electron interaction is sufficiently rapid compared with other processes in the film, the electron system attains a Fermi-Dirac distribution at a temperature T_e. The ensuing loss of energy to the phonon system, together with the modification of the phonon distribution away from the ambient Bose distribution, is characterized by the electron-phonon relaxation time, $\tau_{e\text{-ph}}$, and a time of phonon relaxation, τ_b, towards the substrate temperature. These two relaxation processes act in competition so that phonons for which $\tau_{e\text{-ph}}/\tau_b \gg 1$ remain close to the temperature of the substrate while those for which $\tau_{e\text{-ph}}/\tau_b \ll 1$ will be heated above the temperature of the substrate.

In the original model the mechanism of phonon relaxation was simply phonon loss from the film into the substrate. Several assumptions were made to obtain a simple expression for the rate of phonon escape from the film. First, phonon propagation within the film was ballistic; secondly, the film material was elastically isotropic and thirdly, a reflection coefficient describing the probability of a phonon traversing the film-substrate interface was frequency independent. With these assumptions $\tau_b = 4\eta d/v$, where v is the sound velocity and η is the frequency-independent reflection factor that is equal to the reciprocal of twice the appropriate values of Γ described by Little.[4,8] Hence, in the linear dispersion regime τ_b is independent of the phonon wave vector. The formulation used by Perrin and Budd to describe the frequency dependence of the electron-phonon scattering rate, $\tau_{e\text{-ph}}^{-1}$, was presented by Pippard.[9] This model shows that for a crystalline metal with a spherical Fermi surface, $\tau_{e\text{-ph}}^{-1}$ is proportional to the phonon wave vector. Furthermore, because of the spherical Fermi surface, the interaction only provides coupling between the electrons and longitudinal phonons. From the models for the relaxation times τ_b and $\tau_{e\text{-ph}}$, the wave-vector dependence of $\tau_{e\text{-ph}}/\tau_b$ establishes that high-wave-vector phonons will come into quasiequilibrium with the hot electrons while those of low wave vector will remain close to the temperature of the substrate.

Several experiments[10,11] have shown that at low levels of heater excitation the acoustic-mismatch model and the Perrin-Budd model adequately describe the phonon spec-

trum injected from a metal film into a substrate. However, when the excitation levels are increased, and high phonon frequencies generated, agreement between theory and experiment becomes poor. Using an optical technique, Bron and Grill[11] have analyzed the spectral distribution of a phonon pulse and have shown that the high-frequency components are substantially reduced from the levels predicted by either of the two theoretical models.

More recent studies[12] of phonon generation from metallic films excited at high power levels have also shown attenuation of the high-frequency component of the phonon distribution compared with that predicted by Perrin and Budd. The only explanation consistent with all aspects of the experimental data was that the high-frequency phonons generated within the film underwent strong spontaneous phonon decay before being emitted into the substrate.

In this paper we describe a phonon-radiation model in which we have incorporated spontaneous phonon decay via three-phonon processes as an additional mechanism by which the phonons can relax towards the ambient temperature. It is shown that for an isotropic metal film in the steady state the spontaneous phonon decay modifies the longitudinal-phonon spectrum, produces nonequilibrium transverse-phonon spectra, and reduces the temperature reached by the electrons. We demonstrate that a good correspondence between the calculations and the experimental data exists and that phonon decay in the heater film reduces the need to consider any frequency dependence of the acoustic-mismatch parameter.

MODEL

An analysis of heat-pulse generation requires the solution of coupled electron and phonon transport equations with appropriate boundary conditions at a film-substrate interface. In order to make the problem tractable, we follow the previous work of Perrin and Budd and assume the phonon and electron distributions to be spatially uniform and the exchange of energy between the phonons and the substrate to be described by the relaxation time τ_b. In this approximation the evolution of the phonon distribution $N_j(q)$ is given by

$$\frac{\delta N_j(q)}{\delta t}=\frac{\bar{N}_j(q,T_e)-N_j(q)}{\tau^j_{e\text{-ph}}(q)}+\frac{\bar{N}_j(q,T_0)-N_j(q)}{\tau^j_b}\ , \tag{1}$$

where T_0 is the substrate temperature and $\bar{N}_j(q,T)$ is the Bose distribution of mode j evaluated at temperature T and wave-vector magnitude q. The electron-phonon relaxation rate given by Pippard is

$$[\tau^{\mathrm{L}}_{e\text{-ph}}(q)]^{-1}=\Xi^2 m^2 q/2\hbar^3\pi\rho$$

for the longitudinal mode and

$$[\tau^{\mathrm{T}}_{e\text{-ph}}(q)]^{-1}=0$$

for the transverse modes, where Ξ is the deformation potential, m is the electron mass, and ρ is the mass density. We note, a spherical Fermi surface is considered here.

The model thus far described has only one possible decay channel for the longitudinal-phonon energy, that is via phonon escape to the substrate. We now introduce further terms to take account of the possibility of phonon-energy relaxation via spontaneous phonon-decay processes in the metal films.

The decay of longitudinal phonons in an isotropic solid has been shown[13,14] to proceed via the three processes, $\mathrm{L}\rightarrow\mathrm{L}+\mathrm{T}_2$, $\mathrm{L}\rightarrow\mathrm{T}_1+\mathrm{T}_1$, and $\mathrm{L}\rightarrow\mathrm{T}_2+\mathrm{T}_2$. Each process is governed by the conservation of energy and momentum and has a characteristic relaxation time proportional to q^5 in the Debye model. In this paper we designate the relaxation times $\tau_1(q)$, $\tau_2(q)$, and $\tau_3(q)$ for the three decay processes, respectively. The collinear process $\mathrm{L}\rightarrow\mathrm{L}+\mathrm{L}$ is also possible,[15] but from a final-density-of-states argument the decay rate is small compared with the other processes, and so, we neglect it in the present calculation. The decay of transverse phonons is prohibited in an isotropic solid owing to the conditions of energy and momentum conservation, and is, therefore, disregarded here.

The modification of Eq. (1) to include decay of the longitudinal phonons leads to the following two equations for the longitudinal-phonon distribution,

$$\frac{\delta N_{\mathrm{L}}(q)}{\delta t}=\frac{\bar{N}_{\mathrm{L}}(q,T_e)-N_{\mathrm{L}}(q)}{\tau_{e\text{-ph}}(q)}+\frac{\bar{N}_{\mathrm{L}}(q,T_0)-N_{\mathrm{L}}(q)}{\tau^{\mathrm{L}}_b}+\frac{\bar{N}_{\mathrm{L}}(q,T_0)-N_{\mathrm{L}}(q)}{\tau_1(q)}+\frac{\bar{N}_{\mathrm{L}}(q,T_0)-N_{\mathrm{L}}(q)}{\tau_2(q)}+\frac{\bar{N}_{\mathrm{L}}(q,T_0)-N_{\mathrm{L}}(q)}{\tau_3(q)}\ , \tag{2}$$

$$\frac{\delta N_L(q')}{\delta t}=-\left[\frac{\bar{N}_{\mathrm{L}}(q,T_0)-N_{\mathrm{L}}(q)}{\tau_1(q)}\right]+\frac{\bar{N}_{\mathrm{L}}(q',T_e)-N_{\mathrm{L}}(q')}{\tau_{e\text{-ph}}(q')}+\frac{\bar{N}_{\mathrm{L}}(q',T_0)-N_{\mathrm{L}}(q')}{\tau^{\mathrm{L}}_b}+\frac{\bar{N}_{\mathrm{L}}(q',T_0)-N_{\mathrm{L}}(q')}{\tau_1(q')}$$
$$+\frac{\bar{N}_{\mathrm{L}}(q',T_0)-N_{\mathrm{L}}(q')}{\tau_2(q')}+\frac{\bar{N}_{\mathrm{L}}(q',T_0)-N_{\mathrm{L}}(q')}{\tau_3(q')}\ , \tag{3}$$

where from the conservation laws and to maximize the joint density of final states, $q'=q/2$. The final distribution of longitudinal phonons, therefore, will have two components, one arising from direct generation, the other from the decay $\mathrm{L}\rightarrow\mathrm{L}+\mathrm{T}_2$ for phonons of wave-vector magnitude $q<q_{\mathrm{ZB}}/2$, q_{ZB} being the wave-vector magnitude at the isotropic zone boundary. In addition, the transverse phonons produced by the $\mathrm{L}\rightarrow\mathrm{L}+\mathrm{T}_2$ decay, together with those produced by the last two terms of Eqs. (2) and (3), provide nonequilibrium distributions of

transverse phonons. The evolution of the transverse-phonon distributions can be described by

$$\frac{\delta N_{T_1}(q'')}{\delta t}=\frac{\bar{N}_{T_1}(q'',T_0)-N_{T_1}(q'')}{\tau_b^{T_1}} -2\left[\frac{\bar{N}_L(q,T_0)-N_L(q)}{\tau_2(q)}\right], \tag{4}$$

$$\frac{\delta N_{T_2}(q'')}{\delta t}=-\left[\frac{\bar{N}_L(q,T_0)-N_L(q)}{\tau_1(q)}\right] +\frac{\bar{N}_{T_2}(q'',T_0)-N_{T_2}(q'')}{\tau_b^{T_2}} -2\left[\frac{\bar{N}_L(q,T_0)-N_L(q)}{\tau_3(q)}\right], \tag{5}$$

where $q''=(c/2)q$ with c being the ratio of the longitudinal to transverse velocity of sound. The factors of 2 account for the number of phonons generated in the decay processes $L\rightarrow T_1+T_1$ and $L\rightarrow T_2+T_2$.

The magnitude of the relaxation times τ_1, τ_2, and τ_3 has been the subject of debate for sometime and consequently, the dominant decay channel has been uncertain. Recently, Tamura[16] has reevaluated the magnitude of the spontaneous decay rates for longitudinal phonons in an isotropic solid and has shown that the decay into two transverse-acoustic modes dominates. The decay rates obtained by Tamura have been explicitly presented by Berke *et al.*,[17] and it is from these expressions that we have determined τ_1, τ_2, and τ_3 for this paper.

Solutions for the steady-state phonon distributions are obtained directly from Eqs. (2)–(5),

$$N_L(q)=\frac{1}{1+x(q)}[\bar{N}_L(q,T_e)+x(q)\bar{N}_L(q,T_0)], \tag{6}$$

$$N_L(q')=\frac{\tau_{e\text{-ph}}(q')}{\tau_1(q)}\frac{1}{1+x(q')}\frac{1}{1+x(q)} \times[\bar{N}_L(q,T_e)-\bar{N}_L(q,T_0)] +\frac{1}{1+x(q')}[\bar{N}_L(q',T_e)-\bar{N}_L(q',T_0)] +\bar{N}_L(q',T_0), \tag{7}$$

$$N_{T_1}(q'')=\frac{2\tau_b^{T_1}(q'')}{\tau_2(q)}\frac{1}{1+x(q)}[\bar{N}_L(q,T_e)-\bar{N}_L(q,T_0)] +\bar{N}_{T_1}(q'',T_0), \tag{8}$$

$$N_{T_2}(q'')=\tau_b^{T_2}(q'')\left[\frac{1}{\tau_1(q)}+\frac{2}{\tau_3(q)}\right]\frac{1}{1+x(q)} \times[\bar{N}_L(q,T_e)-\bar{N}_L(q,T_0)]+\bar{N}_{T_2}(q'',T_0),$$

where

$$x(q)=\tau_{e\text{-ph}}(q)\left[\frac{1}{\tau_b^L}+\frac{1}{\tau_1(q)}+\frac{1}{\tau_2(q)}+\frac{1}{\tau_3(q)}\right]. \tag{9}$$

In order to be able to calculate the phonon spectra for a given set of parameters, it is necessary to estimate the steady-state electron temperature for a given applied field E. This is accomplished by considering the energy balance between electrons and the longitudinal phonons given by

$$\frac{E^2}{\rho_{tot}}=\sum_q \hbar\omega(q)\left[\frac{\bar{N}_L(q,T_e)-N_L(q)}{\tau_{e\text{-ph}}(q)}\right], \tag{10}$$

where E is the electric field and ρ_{tot} is the sum of the impurity-limited resistivity ρ_I and the resistivity arising from the phonons.[7] Successive approximations for T_e are made until energy balance is achieved to the accuracy required. The phonon spectra are then calculated for the values of T_e satisfying energy balance.

RESULTS

Using the model described above, we have calculated the longitudinal- and transverse-phonon spectra generated by electrically heating a 10-nm-thick gold film deposited on a sapphire substrate. The equilibrium substrate temperature used was $T_0=7$ k. The following constants were used: electron density $n=6\times10^{28}$ m^{-3}, $\rho_I=5\times10^{-8}$ Ω m, mass density $\rho=19\,300$ kg m^{-3}, and deformation potential $\Xi=3.77$ eV. We also used second-order elastic constants measured at 10 K,[18] $C_{11}=2.0161\times10^{11}$ N m^{-2}, $C_{12}=1.6967\times10^{11}$ N m^{-2}, and $C_{44}=0.4542\times10^{11}$ N m^{-2}, and third-order elastic constants calculated at 0 K,[19] $C_{144}=-1.224\times10^{11}$ N m^{-2} and $C_{456}=-1.561\times10^{11}$ N m^{-2}. Using the method described by Fedorov[20] to define an isotropic medium most similar to the given crystal, we have calculated the sound velocities from the elastic constants and the mass density to be $v_L=3.42\times10^3$ m s^{-1} and $v_T=1.32\times10^3$ m s^{-1}. The resulting phonon-relaxation rates τ_b with[4] $\eta=12.5$ are $(\tau_b^L)^{-1}=0.68\times10^{10}$ s^{-1} and $(\tau_b^{T_1})^{-1}=(\tau_b^{T_2})^{-1}=0.26\times10^{10}$ s^{-1}. The magnitude of the isotropic zone-boundary wave vector, q_{ZB}, for gold was estimated from the low-temperature lattice constant of 0.395 nm and the fcc structure, to be 1.72×10^{10} m^{-1}.

The longitudinal-phonon energy-density distribution, $q^3N_L(q)$ generated with an electric field of 1.55×10^5 V m^{-1} is shown in Fig. 1 (curve 1) together with the energy density calculated without the inclusion of spontaneous decay (curve 2). The most prominent difference between the two spectra occurs for wave vectors above $q_{ZB}/2$. Down-conversion reduces the energy density of phonons close to the zone boundary by approximately 2 orders of magnitude and produces a maximum in the spectrum at a wave vector slightly below $q_{ZB}/2$. We note that because the spontaneous decay provides a mechanism for energy to be lost from the longitudinal to the transverse modes, the longitudinal-phonon energy density calculated with down-conversion always lies completely below the energy density calculated by the original Perrin-Budd model. The corresponding energy density $q^3N_T(q)$ for the transverse modes T_1 (curve 1) and T_2 (curve 2) is shown in Fig. 2. The high-wave-vector part of the spectrum ($q>2\times10^9$ m^{-1}) is generated by down-

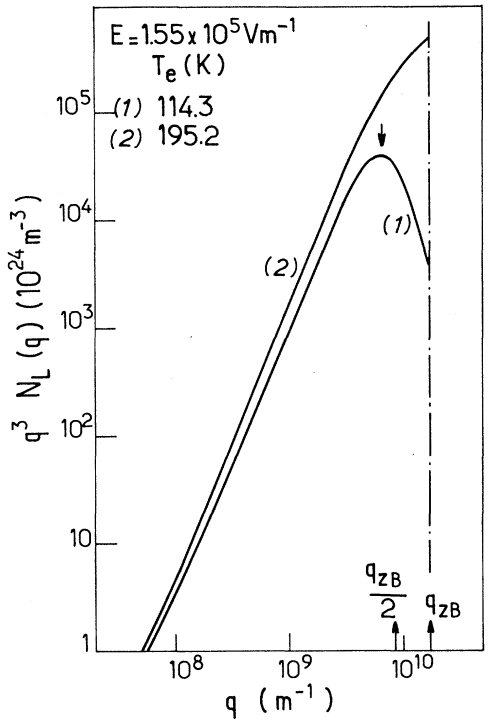

FIG. 1. The longitudinal-phonon energy-density distribution calculated with [curve (1)] and without [curve (2)] three-phonon processes.

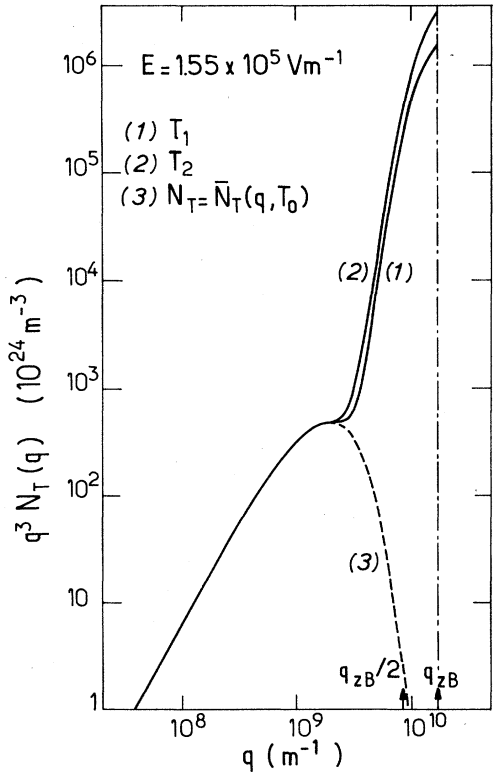

FIG. 2. The transverse-phonon energy-density distribution for a field of 1.55×10^3 V m^{-1}. The T_1 and T_2 modes are shown in curves (1) and (2), respectively, and curve (3) shows the transverse-phonon distribution at the ambient temperature.

conversion of the longitudinal phonons, whereas the low-wave-vector part corresponds to the equilibrium distribution $\bar{N}_T(q,T_0)$ at T_0. The equilibrium energy spectrum at high wave vectors is shown by the dashed curve (3) in Fig. 2.

The differences between the longitudinal-phonon energy-density spectra with and without down conversion can be understood by considering the various relaxation rates in the problem. Using the constants given above, we estimate that $(\tau_b^L)^{-1}=0.68\times10^{10}$ s^{-1} and $\tau_{e\text{-ph}}^{-1}=2.1q$ s^{-1}. From the expressions given by Berke *et al.*, we calculate that $\tau_1^{-1}=7\times10^{-41}q^5$ s^{-1}, $\tau_2^{-1}=2\times10^{-40}q^5$ s^{-1}, and $\tau_3^{-1}=4\times10^{-40}q^5$ s^{-1} showing that the $L\rightarrow T_2+T_2$ is the dominant three-phonon process. For wave vectors close to the zone center $(\tau_b^L)^{-1}>\tau_{e\text{-ph}}^{-1}>\tau_3^{-1}$, therefore, the phonons generated by the electrons escape from the film without undergoing spontaneous decay. In this limit the present model agrees with the original Perrin-Budd model as shown in Fig. 1. In the wave-vector regime where $(\tau_b^L)^{-1}<\tau_{e\text{-ph}}^{-1}<\tau_3^{-1}$, the phonons are generated and escape at a rate below that of spontaneous decay; thus, all of the phonons decay before they are able to leave the heater film. This situation exists for phonons of wave vector above 8.5×10^9 m^{-1}, that is $q_{ZB}/2$, and so, in this region we expect the greatest difference between the models with and without spontaneous phonon decay.

The longitudinal- (L) and transverse- (T_1,T_2) phonon energy-density spectra, and the total energy-density spectrum (Σ), including both the longitudinal and transverse modes, are shown in Fig. 3 for an electric field $E=1.55\times10^5$ V m^{-1}. The important contribution of the transverse modes to the total energy spectrum is easily seen from this figure. The low-frequency part of the transverse-phonon energy spectra (curve T) is the equilibrium distribution $\bar{N}(\omega,T_0)$ at T_0. A nonequilibrium spectrum for the transverse phonons appears for $\omega\sim3\times10^{12}$ s^{-1}. The transverse-mode energy spectra are larger than that of the longitudinal mode, except in a small region about the maximum where the nonequilibrium transverse spectra appear. This is in fact due to the higher density of states of the transverse phonons, as can be seen from Fig. 4 where the corresponding phonon distributions $N_j(\omega)$ for the mode j are shown. At large frequencies $\omega>3\times10^{12}$ s^{-1}, the transverse-phonon equilibrium distribution is very small [curve (5)]; thus, the minimum observed in the T_1 and T_2 distributions [curves (3) and (4)] is due to the occurrence of down-conversion. A maximum is also observed in these curves: it results from the low value of the distribution of the longitudinal phonons that can be down-converted at high frequency [curve (1), $\omega_{ZB}/2<\omega<\omega_{ZB}$]. Around this maximum, the transverse-mode distributions are larger than the longitudinal distribution which indicates the importance of down-conversion; this is also seen by comparing the curves (1) and (2) that represent the longitudinal-phonon distributions without [curve (1)] and with [curve (2)] down-conversion.

We have also investigated the dependence of the longitudinal-phonon energy-density distribution on the applied electric field. The wave-vector dependence of $\tau_{e\text{-ph}}$ shows that hot electrons tend to relax by emitting

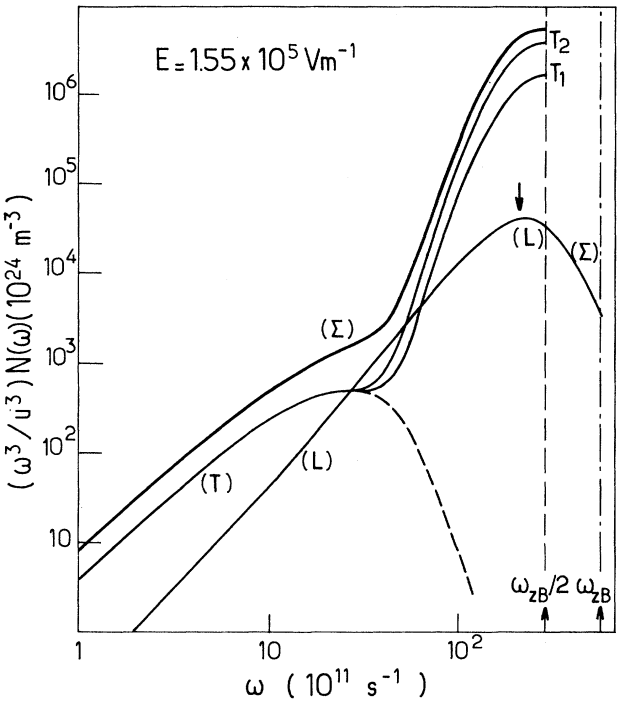

FIG. 3. The longitudinal (L) and transverse phonon (T_1,T_2) energy densities together with the total energy-density spectrum (Σ). ω_{ZB} is the angular frequency of the longitudinal mode at the zone boundary.

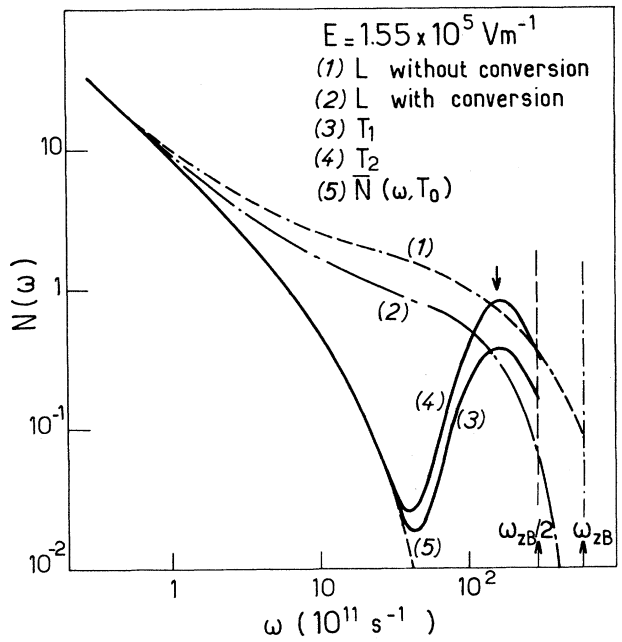

FIG. 4. The frequency distributions for the longitudinal and transverse phonons for a field of 1.55×10^5 V m^{-1}.

phonons of high wave vector. In the original Perrin-Budd model this effect was manifest by the peak of the phonon-energy density distribution increasing from the maximum of the ambient-temperature Bose-Einstein distribution to higher wave vectors as the electric field was increased. Further increases in the field caused the maximum to continue to move to higher wave vectors and approach the zone boundary.[12] We have found this behavior to be modified in the presence of spontaneous phonon decay. The energy-density distributions of longitudinal phonons for several values of the electric field are shown in Fig. 5. As expected, the three-phonon processes reduce the energy density for phonons of wave vector above $q_{ZB}/2$. We note that the energy-density curve obtained for the lowest field considered, 10^3 V m^{-1}, hardly differs from the corresponding curve without down-conversion at wave vectors greater than 5×10^9 m^{-1} (dashed curve). The peak of the distribution as a function of electric field is shown in Fig. 6. In the presence of three-phonon processes, as the electric field is increased from zero, the maximum of the energy density follows the original model up to fields $\sim2\times10^3$ V m^{-1}. At higher fields the position of the maximum becomes less dependent on the electric field and approaches a value of $q_{ZB}/2$. An interpretation of this behavior is relatively straightforward; as the electron temperature is increased by the field, higher-energy phonons are emitted. The q^5 wave-vector dependence of the three-phonon processes makes spontaneous decay more effective at high fields, and so, the large-wave-vector phonons emitted by the electrons rapidly down-convert before being able to leave the film.

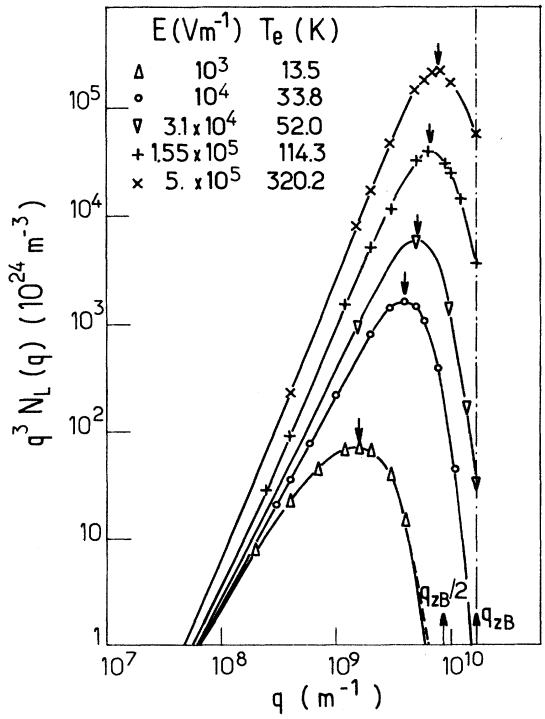

FIG. 5. The energy-density distribution of the longitudinal phonons for several electric fields.

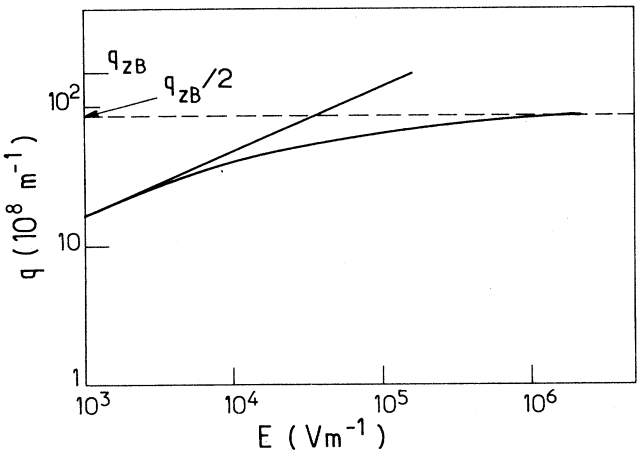

FIG. 6. The dependence of the magnitude of the wave vector corresponding to the peak in the energy density, as a function of electric field. The straight line indicates the dependence in the absence of three-phonon processes.

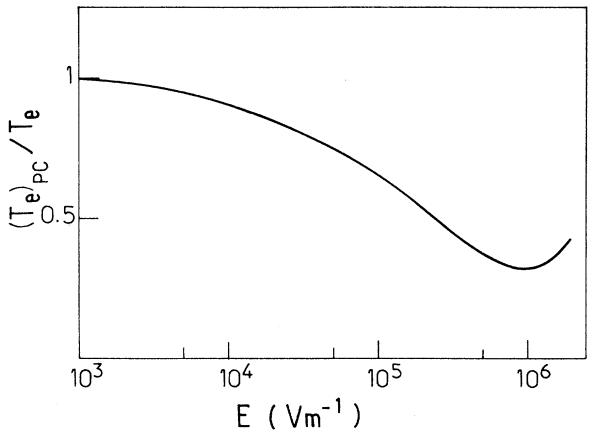

FIG. 7. The ratio of the steady-state electron temperatures with and without the three-phonon processes, as a function of electric field.

From the condition of power balance we have also been able to determine the steady-state electron temperature for a given electric field. To illustrate the effect spontaneous phonon decay has on the electron temperature, we have calculated the ratio of the steady-state electron temperature $(T_e)_{PC}$ with phonon decay to the electron temperature T_e without phonon decay, Fig. 7. At the lowest electric fields, the electron temperature is close to that found by Perrin and Budd. However, as the field is increased, the ratio falls until at high fields it goes through a minimum. We note that the field at which the ratio of electron temperatures starts to decline is the same field at which the dependence of the energy-density maximum begins to deviate from the original Perrin-Budd model. The high-field electron-temperature behavior results from the increased electron scattering that increases the resistivity of the metal. When the down-conversion is not considered, this leads to a value of T_e, for a given electric field, smaller than the value obtained with resistivity determined by the impurities only [Eq. (10)].

Finally, we briefly compare the results of our calculations with some experimental data. The spectroscopic studies of Bron and Grill[11] showed that a heat pulse emitted from a thin metal film contained fewer high-frequency phonons than predicted by Perrin and Budd. Bron and Grill put forward an interpretation of the discrepancy based on the fact that the frequency-independent acoustic-mismatch model was breaking down for phonons whose wavelengths approached atomic dimensions. The present calculations indicate that phonon down-conversion in the metal films is sufficient to account for the reduced numbers of high-frequency phonons. Furthermore, the present model suggests that the majority of phonons impinging on the film-substrate interface are of a wavelength greater than atomic dimensions; consequently, the frequency-independent acoustic-mismatch approximation is expected to be valid in this case. We note that in a real metal-film heater, mode softening near the zone boundary will cause the down-conversion of near-zone-boundary phonons to become even more efficient since their escape time will be increased. Moreover, in the real situation high-frequency phonons will be more strongly scattered at the film-substrate interface which will further increase their escape time. A more detailed analysis of the similarities between the present work and the data of Bron and Grill is inappropriate since the heater and substrate materials used in their experiments were substantially different than those considered here.

A closer comparison may be made with recent phonon-pulse data obtained using thin gold-palladium films deposited onto a carefully prepared sapphire substrate.[12] The films were excited using electric fields of up to $3\times10^5\ V\,m^{-1}$ for durations on the nanosecond time scale. As a result of the short excitation time, large power densities were achieved and a significant population of phonons was produced at the zone boundary of the metal film. By detecting the dispersive broadening of the phonon pulse launched into the substrate, the wave vector of the dominant phonons within the longitudinal pulse was estimated to be $q_{ZB}/2$ which is in agreement with the present analysis, Fig. 5. Moreover, the experiments showed that as the electric field was reduced, the ratio of the number of transverse to longitudinal phonons fell: this result is consistent with the transverse-phonon spectra being generated by spontaneous three-phonon decay.

ACKNOWLEDGMENTS

One of the authors (M.N.W.) would like to thank the Groupe de Physique des Solides de l'Ecole Normale Supérieure, Paris, for their kind hospitality during the preparation of this work. M.N.W. also acknowledges that part of this work was supported by the U.S. National Science Foundation under Grant No. DMR-87-13884.

[1]R. J. von Gutfeld, in *Physical Acoustics V,* edited by W. P. Mason (Academic, New York, 1968), p. 223.
[2]G. A. Northrop and J. P. Wolfe, in *Nonequilibrium Phonon Dynamics,* edited by W. E. Bron (Plenum, New York, 1985), p. 165.
[3]See references in M. N. Wybourne and J. K. Wigmore, Rep. Prog. Phys. **51**, 923 (1988).
[4]W. A. Little, Can. J. Phys. **37**, 334 (1959).
[5]H. J. Maris, J. Phys. (Paris) Colloq. **33**, C4-3 (1972).
[6]N. Perrin and H. Budd, Phys. Rev. Lett. **28**, 1701 (1972).
[7]N. Perrin and H. Budd, J. Phys. (Paris) Colloq. **33**, C4-3 (1972).
[8]O. Weis, Z. Angew. Phys. **26**, 325 (1969).
[9]A. B. Pippard, Philos. Mag. **46**, 1104 (1955).
[10]P. Herth and O. Weis, Z. Angew. Phys. **29**, 101 (1969).
[11]W. E. Bron and W. Grill, Phys. Rev. B **16**, 5303 (1977).
[12]M. N. Wybourne, J. K. Wigmore, and N. Perrin, J. Phys. Condens. Matter **1**, 5347 (1989).
[13]R. Orbach and L. A. Vredevoe, Physics **1**, 91 (1964).
[14]P. G. Klemens, J. Appl. Phys. **38**, 4537 (1967).
[15]S. Simons, Proc. R. Soc. London **82**, 401 (1963).
[16]S. Tamura, Phys. Rev. B **31**, 2575 (1985).
[17]A. Berke, A. P. Mayer, and R. K. Wehner, J. Phys. C **21**, 2305 (1988).
[18]J. R. Neighbours and G. A. Alers, Phys. Rev. **111**, 707 (1958).
[19]B. P. Barua and S. K. Sinha, J. Appl. Phys. **49**, 3967 (1978).
[20]F. I. Fedorov, *Theory of Elastic Waves in Crystals* (Plenum, New York, 1968), Chap. 5.